metals

MDPI

Article

Use of the Swebrec Function to Model Particle Size Distribution in an Industrial-Scale Ni-Co Ore Grinding Circuit

Alfredo L. Coello-Velázquez [1], Víctor Quijano Arteaga [1], Juan M. Menéndez-Aguado [2,*], Francisco M. Pole [3,4] and Luis Llorente [5]

1 CETAM, Universidad de Moa Dr. Antonio Núñez Jiménez, Bahía de Moa 83300, Cuba
2 Escuela Politécnica de Mieres, Universidad de Oviedo, Mieres 33600, Spain
3 Escola Superior Politécnica da Lunda Sul, Universidade Lueji A'Nkonde, Saurimo 161, Angola
4 Sociedade Mineira de Catoca Lda., Luanda 10257, Angola
5 Empresa Comandante Ernesto Ché Guevara., Punta Gorda 83310, Cuba
* Correspondence: maguado@uniovi.es; Tel.: +34-985-458-033

Received: 9 July 2019; Accepted: 8 August 2019; Published: 10 August 2019

Abstract: Mathematical models of particle size distribution (PSD) are necessary in the modelling and simulation of comminution circuits. In order to evaluate the application of the Swebrec PSD model (SWEF) in the grinding circuit at the Punta Gorda Ni-Co plant, a sampling campaign was carried out with variations in the operating parameters. Subsequently, the fitting of the data to the Gates-Gaudin-Schumann (GGS), Rosin-Rammler (RRS) and SWEF PSD functions was evaluated under statistical criteria. The fitting of the evaluated distribution models showed that these functions are characterized as being sufficiently accurate, as the estimation error does not exceed 3.0% in any of the cases. In the particular case of the Swebrec function, reproducibility for all the products is high. Furthermore, its estimation error does not exceed 2.7% in any of the cases, with a correlation coefficient of the ratio between experimental and simulated data greater than 0.99.

Keywords: comminution; grinding circuit; Swebrec function; size distribution models; modelling; lateritic ore

1. Introduction

The particle size distribution (PSD) in granular materials is one of the quality indicators of many transformation processes. In the particular case of mining, it is a measure of effectiveness [1] from blasting operations through to comminution. It is a crucial element of control in the processing of materials. In the specific case of the Punta Gorda milling plant (Moa, Cuba), P80 governs the quality of the final product, together with P95 and P70, product sizes which should correspond to 149 µm, 74 µm and 44 µm, respectively.

The Punta Gorda industrial plant processes lateritic minerals from deposits in northeastern Cuba by means of the ammonium-carbonate technology to obtain nickel and cobalt concentrates. Grinding plays an important role in this technological context, ensuring an adequate contact surface of the ore to allow the reduction of nickel and cobalt to their metallic phases and the subsequent solution of these elements in the leaching process [2–5]

The mathematical representation of the PSD is a mandatory tool in the modelling and simulation of processes, in addition to being crucial for controlling efficiency in comminution circuits. In most existing PSD models, the particle size is plotted against the cumulative undersize [6], p representing the probability that a fragment is smaller than x, the particle size.

In ore processing, PSD can be obtained directly through sieve analysis, or indirectly via the processing of a digital image and the use of sensors based on artificial neural networks [7–9].

Ouchterlony [10,11] argues that these techniques based on image processing have many drawbacks, one of which is the tendency to provide incorrect shapes of the size distribution curves. Therefore, the integration of PSD models in the different ways in which particle sizes are experimentally determined and the determination of the parameters of these functions is both a straightforward and satisfactory means of characterization, control and automation in comminution processes.

In comminution and mechanical separation processes, the PSD is limited to the determination of the F80 feed size and P80 product size diameters, as likewise occurs in the standard tests to determine the Bond index [12]. In many cases, the process engineer uses the graphic method for this purpose. This behaviour can have serious consequences in decision-making in the operation and control of comminution and mechanical concentration processes.

The aim of the present study is to present the potential advantages of applying the Swebrec (SWEF) function [10] in the modelling of the PSD of the products of the dry grinding circuit of lateritic minerals.

1.1. Models of Particle Size Distribution

In practice, the most widespread PSD models in ore processing are two-parameter mathematical functions, one parameter being the size coefficient and the other, the distribution coefficient [13].

The Rosin-Rammler model (RRS) is usually considered the best size distribution model for ore processing applications, although the Gates-Gauss-Schumann distribution (GGS) is preferred in certain applications such as coal processing, especially in North America [9]. Álvarez Rodríguez et al. [12] concluded that it is preferable to use the RRS model to determine the F80 and P80 diameters in the Bond ball mill test.

For the characterization of the PSD of blast fragmentation, Blair [14] obtained excellent results with the two-parameter logarithmic function for particles smaller than 0.1 mm; however, the worst results were obtained using the RRS function. For this case, the fragmentation function that provided the best fit was based on the Kuz-Ram model [15]. Other models exist, such as the two-parameter model proposed by Djordjevic [16] and the crush zone model [17], which were developed for the particle size characterization of blast fragmentation [6]. There are no known applications of these models in ore processing.

The main drawbacks of the larger models in ore processing (GGS and RRS) reside in the respective expansions and contractions of certain regions of the curve.

1.2. Swebrec Function

The Swebrec function (SWEF), proposed by Ouchterlony [10,18], is given by Equation (1):

$$P(x) = \frac{1}{1 + \left[\frac{\ln\left(\frac{x_{max}}{x}\right)}{\ln\left(\frac{x_{max}}{x_{50}}\right)}\right]^{b}} \quad (1)$$

where:

- $P(x)$, cumulative undersize, u
- x_{max}, maximum size of ore particles, mm.
- x, size, mm.
- x_{50}, sieve size that retains 50% of the material, mm.

Unlike the most commonly used models in ore processing, this is a three-parameter size distribution model. The parameters are: x_{max}, x_{50} and b. When $b = 1$, the inflection point tends towards $x = x_{max}$ and when b increases to 2, the inflection point tends towards $x = x_{50}$.

2. Methodology

Data were obtained by carrying out a full factorial experiment in the dry grinding circuit at the Punta Gorda plant. In this experiment, eight trials were devised with different operating conditions. Three operational variables were studied: ore feed flow (*t*/*h*), air flow rate to the mill (m^3/h) and the position of the air separator vanes (*u*), with a 45% ball load in all cases. The base levels of the variables were: 100 *t*/*h*; 68700 m^3, and 5, respectively.

Primary samples were taken every 15 min in each operating mode, which had a duration of 8 h. The samples were subjected to sieving analysis to determine the particle size composition: up to 1 mm dry, and below 1 mm wet. The following sieves were used for the fresh feed material: 40.0, 25.0, 18.0, 12.0, 10.0, 6.0, 4.75, 3.5, 2.0, 1.25, 1.0, 0.6, 0.4, 0.2, 0.1, and 0.074 mm. For the recirculated product in the mill, the product discharged from the mill and final product of the circuit, the following sieve sizes were used: 0.149; 0.074, and 0.044 mm.

The resulting data were subjected to the Coello procedure [19] in order to avoid the effect of fluctuations in the characteristics and properties of the fresh material, and errors and anomalous variations in the size class balance. Results are shown in Appendix A (Tables A1–A3).

The experimentally obtained PSDs of the different products of the milling circuit were fitted to the GGS, RRS and SWEF models according to the procedures set out in [6,9,11]. The coefficient of determination, the estimation error and Cochran's criterion were used as quality criteria for the fitting. The procedures were run with the help of Excel software templates prepared for such purposes. Considering the results of the values of the Cochran and Chi-Square criteria, the average values of the experiment were presented for each size distribution function.

3. Results and Discussion

3.1. Balance of the Size Class Distribution of the Grinding Circuit Minimizing Residual Errors

A simplified closed circuit scheme of lateritic ore comminution similar to that used in the grinding plant at the Punta Gorda nickel processing plant is presented in [19,20].

The results of calculating the circulating load per equation by means of the conventional equation appear in Table A1. As a result of the inherent fluctuations in the technological process, above all at the scale at which the sampling took place, the values of the residuals vary considerably (Table A2), by both excess and defect.

Table A3 shows the recalculated values of the circulating load and the PSD whose residual in the class balance is zero. This means that the newly found values of the particle size distribution better satisfy the calculation of the circulating load and hence the general balance of the particle size distribution of the size classes.

3.2. Fresh Feed to the Mill

Figure 1 shows the results of the particle size distribution of the fresh feed product to the mill.

In general, the experimental PSD occupies an intermediate position between the RRS and SWEF distributions. A more detailed analysis shows that for particles larger than 10 mm, the experimental data is closer to the RRS distribution; i.e., this function provides a better fit to the experimental data in this region of the curve. The mass fraction corresponding to this coarse class (>10 mm) is approximately 8%.

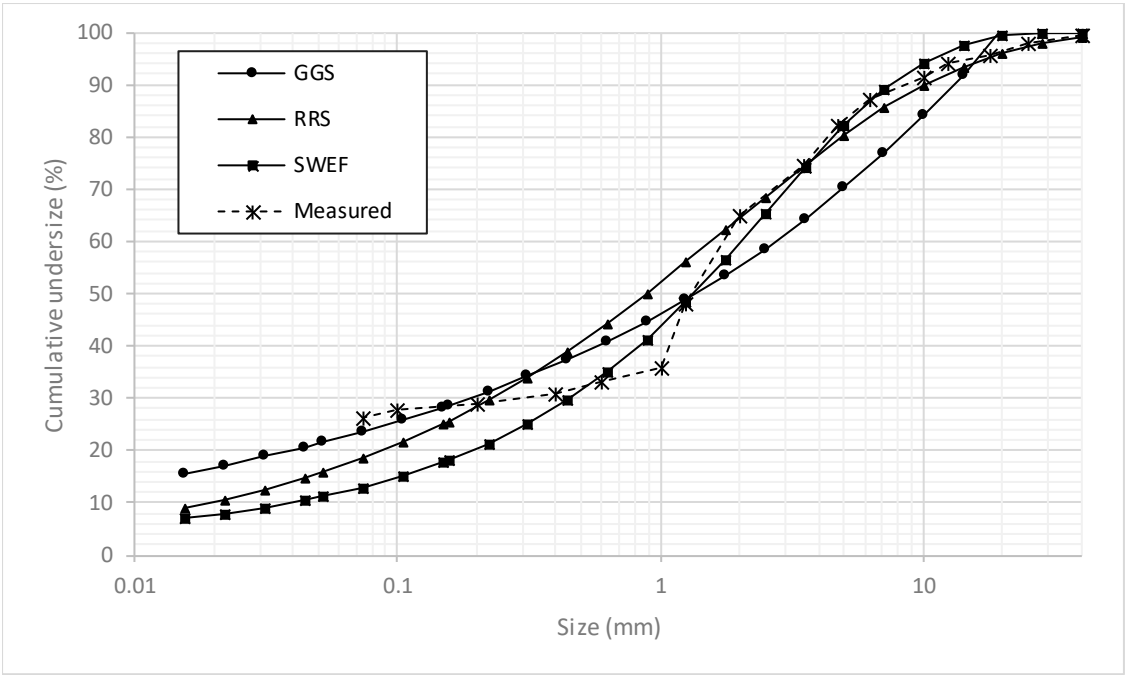

Figure 1. Size distribution of the ore particles of the fresh feed to the mill.

The region of the experimental distribution between sizes below 6–8 mm behaves very differently, however. This region is closer to the distribution of the SWEF, and accounts up to 87% of particles. In short, the RRS function best describes the coarse size ranges, while the SWEF better fits the experimental data in the fine fractions.

According to the R^2 values, the SWEF provides the best fit, the value of its coefficient of determination, R^2, being lower than those presented by Ouchterlony [1] for products of fragmentation by blasting and crushing. It should be noted that the fresh feed to the mill did not undergo any comminution operation after it was mined, although this product was influenced by the operations of mining, loading, transport, unloading and drying. Therefore, it may be considered a run-of-mine material. As to the value of coefficient b, in this case it does fit the range of values reported by Sanchidrián et al. [6], although it is slightly higher than the values of b reported for crushing.

It can be seen in Figure 2 that only four values are separated to some extent from the zero error line, which is an indicator of a good fit of the experimental data to the Swebrec function.

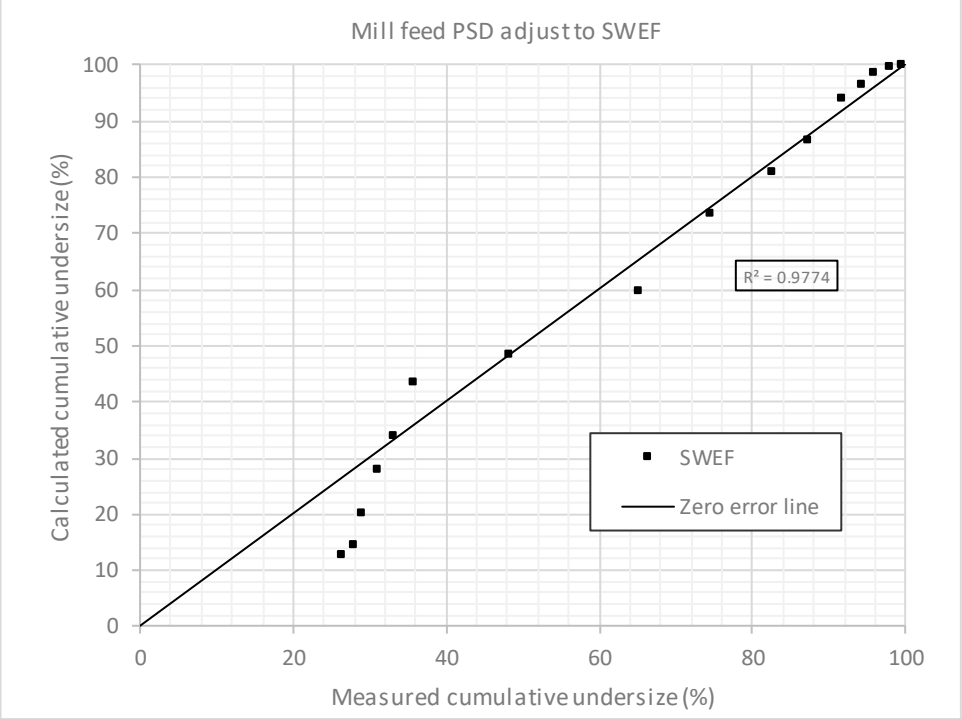

Figure 2. Zero error graph for the SWEF.

3.3. Mill Discharge

Figure 3 shows the particle size distribution of the mill discharge fitted to the PSD models studied in this paper. As can be seen in the figure, the SWEF occupies an intermediate position between the GGS and RRS distributions for sizes between 35 and 7 microns. For sizes below 7 μm and between 35 μm and 149 μm, the SWEF distribution respectively approaches the GGS and RRS distribution functions.

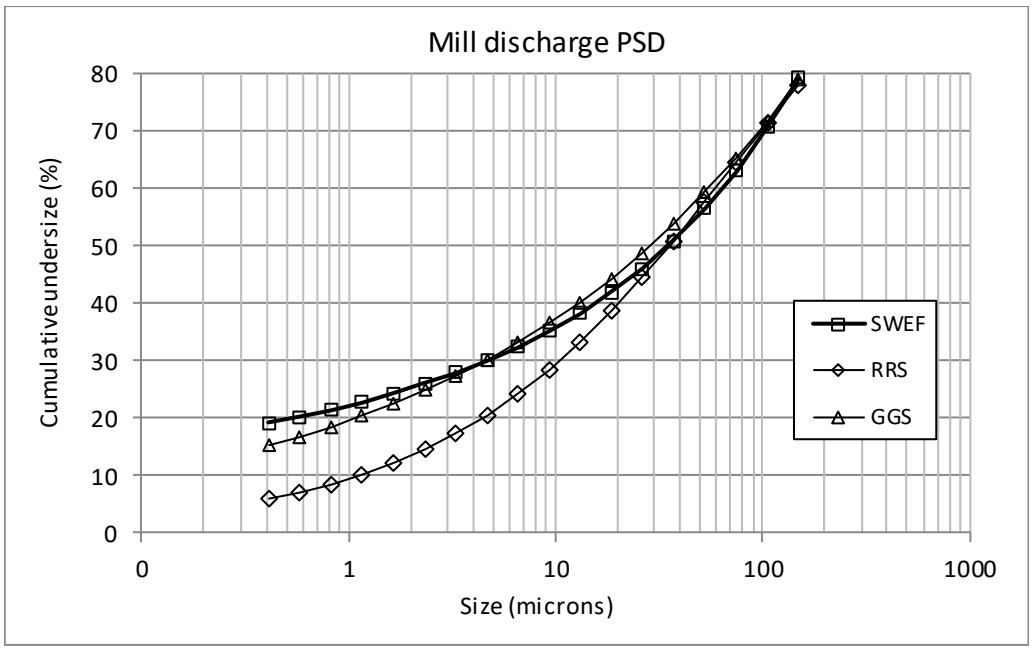

Figure 3. Particle size distribution simulated by the models under study.

The reported value of b (Table 1) falls within the range of values reported in [6], although it is somewhat lower than the value of b reported for fresh feed to the mill. The R^2 is higher than that obtained for the latter product. Considering the value of the estimation error (σ), the best fit corresponds to the SWEF model. The coefficient of determination for the experimental data and those simulated by the SWEF model is 0.9999 (Figure 4).

Table 1. Studied model parameters, mill discharge.

MDTP	Model Parameters					R^2	σ
	Slope, m	K (*)	X_{max}	X_{50}	b		
GGS	0.2792	0.3461	-	-	-	0.9867	2.14
RRS	0.5425	0.0703	-	-	-	0.9867	3.04
SWEF	-	-	0.3461	0.0353	1.3354	0.9927	1.77

(*) $d_{62.8}$—for RRS and d_{100}—for GGS.

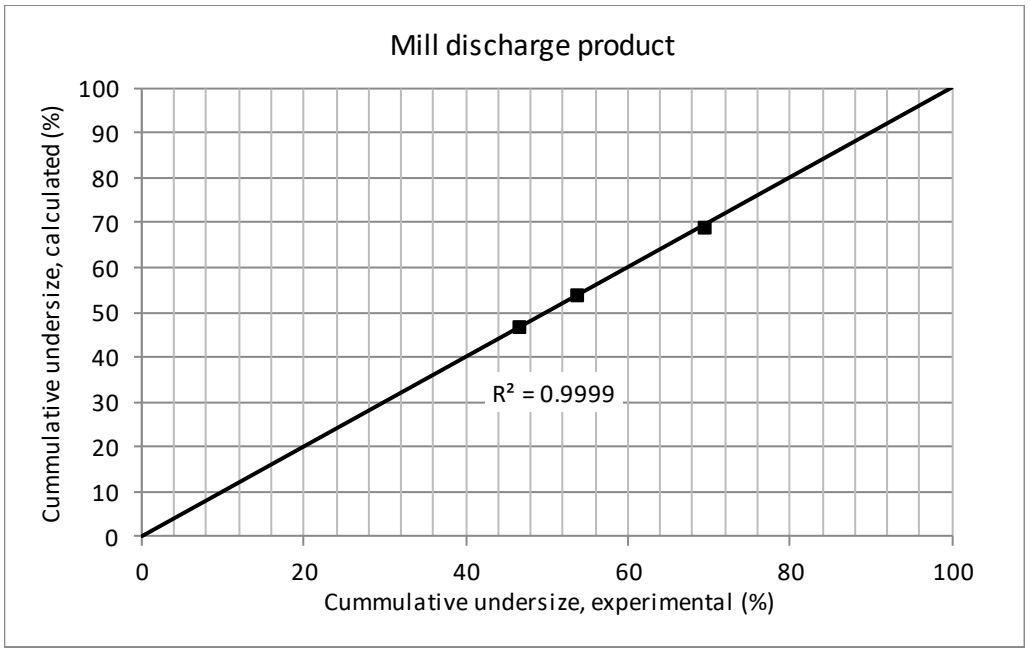

Figure 4. Zero error graph for the mill discharge.

The calculated Cochran criterion (0.2858) is lower than the critical criterion (0.6798), which indicates good homogeneity in the error made in the experimentation and the absence of significant differences between the series of experimental data and the data simulated by this function. It was similar for the other distributions under study.

3.4. Recirculated Product in the Mill

Figure 5 shows the size distribution of the product recirculated in the grinding circuit at the Punta Gorda plant fitted to the GGS, RRS and SWEF models.

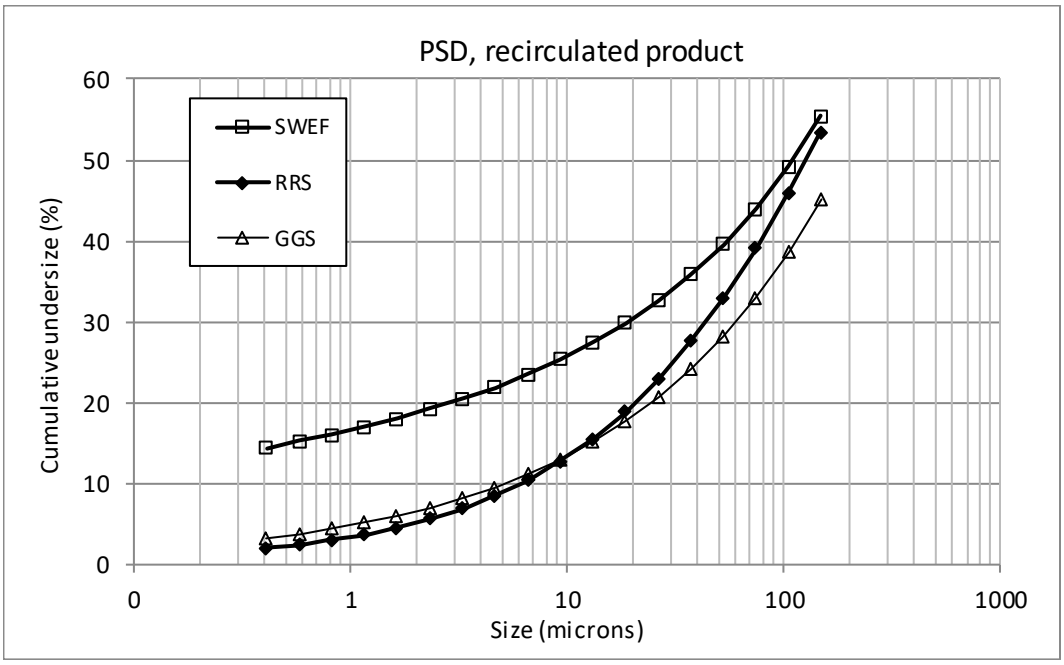

Figure 5. Particle size distribution of the product recirculated in the grinding circuit.

The configuration of the particle size distribution curve is similar to that of the mill discharge, the value of b = 1.3206 being very similar (see Tables 1 and 2).

Table 2. Parameters of the distribution models under study, recirculated product.

MDTP	Model Parameters					R^2	σ
	Slope, m	K *	X_{max}	X_{50}	b		
GGS	0.4507	0.8732	-	-	-	0.9605	1.9277
RRS	0.6224	0.2299	-	-	-	0.9538	2.1163
SWEF	-	-	0.7787	0.1104	1.3206	0.9743	2.6468

(*) $d_{62.8}$—for RRS and d_{100}—for GGS.

The curve of the Swebrec function is always above the other distribution models, tending to approach the curve of the RRS distribution. This function occupies precisely the intermediate position.

For this product, the SWEF distribution shows the best-fit parameter value, although the estimation error is greater than in the other two distributions. However, the error is lower than 2.7% and it may be stated that the SWEF characterizes the particle size distribution of the mill discharge with sufficient accuracy.

Figure 6 shows the zero error graph for the case of the recirculated product. It includes the coefficient of determination, which in this case is 0.9925, thus confirming the model's suitability. The calculated Cochran criterion is lower than the critical criterion (0.6088 versus 0.6798).

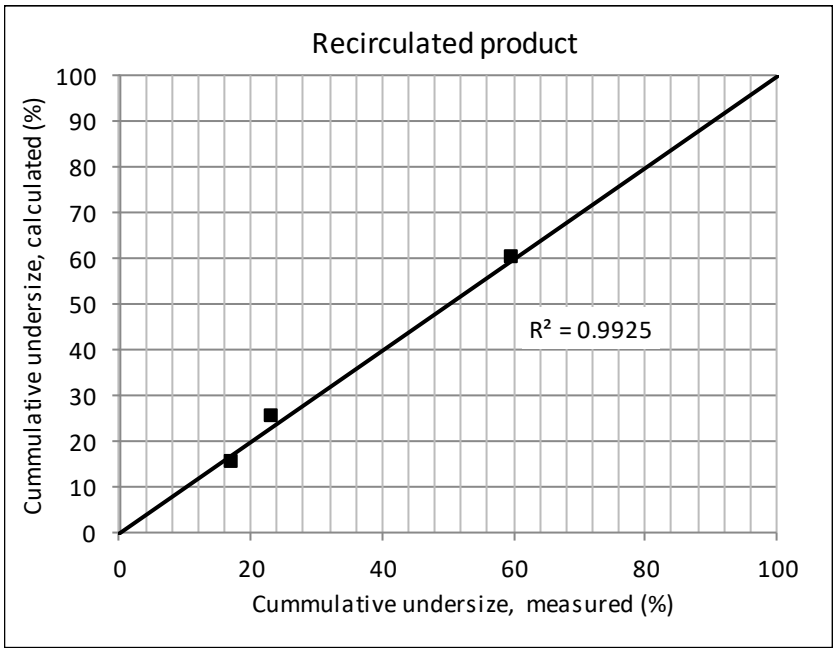

Figure 6. Zero error graph, recirculated product fitted to the SWEF model.

3.5. Final Product of the Circuit

The fitting of the size distribution functions evaluated in this paper is presented in Figure 7. The SWEF occupies an intermediate position between the other two studied distributions, tending to parallel the GGS model to a certain extent. Here, the RRS distribution behaves quite differently from the other two models towards the finer fractions, although all of the functions converge from 37 μm to the coarser classes. The estimation error does not exceed 2.5% for any of the functions.

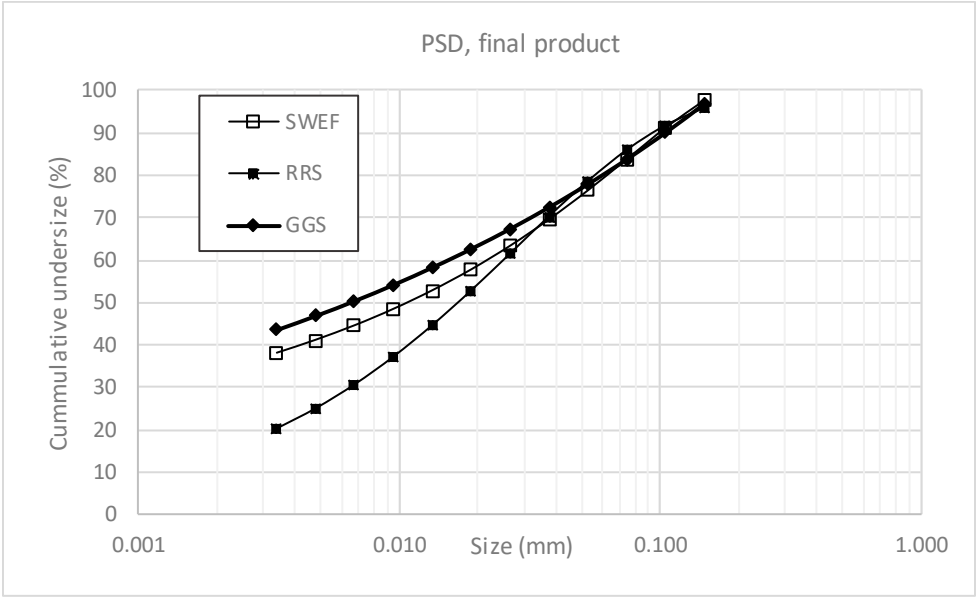

Figure 7. Distribution models fitted to the experimental data.

The value of coefficient *b* is somewhat greater than coefficient *b* of the size distributions of the products discharged from and recirculated in the mill. This justifies the similar behaviour of the SWEF distribution model for these products.

As expected, the maximum size in the distribution is lower than that of the other products. Something similar occurs with the x_{50} size, which constitutes the cut-off size of the pneumatic separator.

The zero error graph (Figure 8) confirms the reproducibility of the SWEF model. The coefficient of determination of the experimental data and the data simulated by this model is 0.9925. The values of the calculated Cochran criterion and the critical criterion (0.2858 versus 0.6798) confirm the high quality of the model.

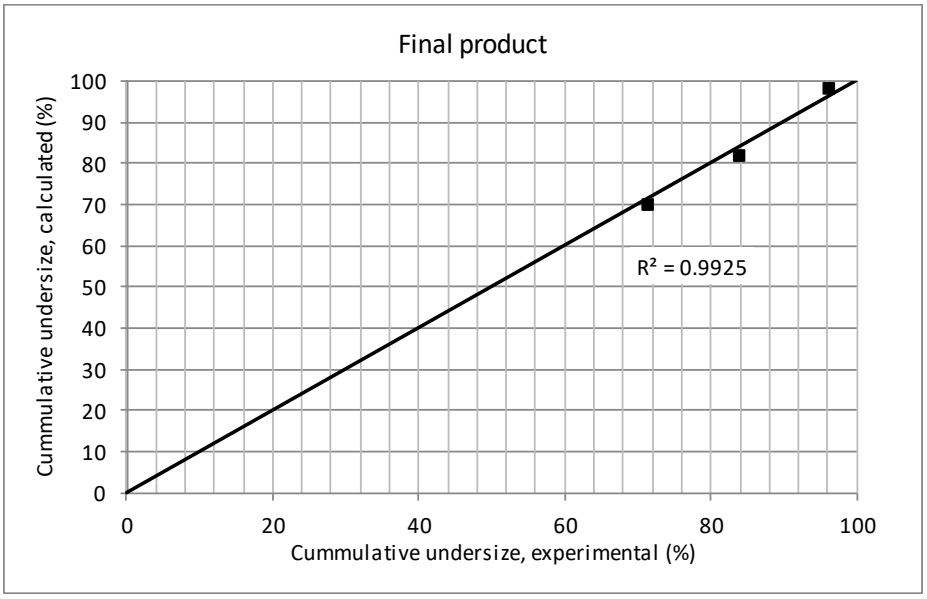

Figure 8. Zero error graph of the experimental data and the data simulated by the SWEF.

Figure 9 shows the PSDs of the different products of the grinding circuit simulated by the Swebrec function for normalized sizes with a sieving scale of $\sqrt{2}$. The shape of the distribution for the products inside the circuit is similar, the tendency following the logic of the x_{max} and x_{50} sizes reported in Tables 1–4.

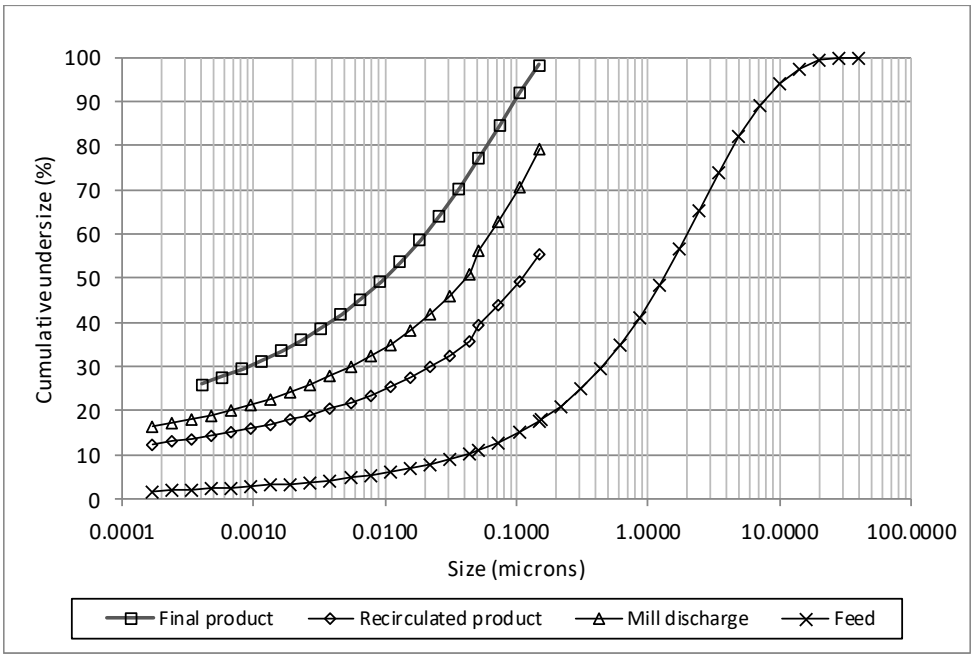

Figure 9. Simulation of the particle size distribution for products in the grinding circuit.

Table 3. Parameters of the distribution models under study.

Model	Model Parameters					R^2
	Slope, m	K (*)	X_{max}	X_{50}	b	
GGS	0.2493	0.429	-	-	-	0.900
RRS	0.3352	1.857	-	-	-	0.954
SWEF	-	-	40.0	1.331	3.10	0.977

(*) $d_{62.8}$ for RRS and d_{100} for GGS.

Table 4. Parameters of the distribution models for the final product of the circuit.

MDTP	Model Parameters					R^2	σ
	Slope, m	K (*)	X_{max}	X_{50}	b		
GGS	0.2026	0.1690	-	-	-	0.9763	1.4051
RRS	0.7489	0.0284	-	-	-	0.9869	1.1234
SWEF	-	-	0.1749	0.0099	1.401	0.9855	2.2193

(*) $d_{62.8}$ for RRS and d_{100} for GGS.

4. Conclusions

The results of applying the Coello procedure [19] allowed us to obtain the particle size distribution of the different products of the milling circuit suitably balanced with zero residual values.

For all the size distributions, no significant differences were found between the experimental data and the data simulated by the size distribution models. In combination with the values obtained from the coefficient of determination and the estimation error, this means that all the studied models are reproducible. The Cochran criterion and Chi-square values confirm the above: the calculated values are always better than the critical values of the considered statistics.

The Swebrec function characterizes the particle size distribution of the products of the grinding circuit very accurately. The coefficient of determination for the experimental data and those simulated by the model is greater than 0.9900. The average error of its fitting to the size distribution of the products of the grinding circuit does not exceed 3%, demonstrating the versatility of its use. The coefficient of determination values for the experimental data and those simulated by this function are predominantly very high.

The b value for the products inside the grinding circuit ranges between 1.32 and 1.4. The b value for the fresh feed (crushed product) coincides with the values reported by Sanchidrián et al. [6] for crushing.

Author Contributions: Conceptualization, J.M.M.-A., A.L.C.-V.; Formal analysis, V.Q.A. and F.M.P.; Investigation, F.M.P. and R.M.A.; Methodology, A.L.C.-V. and J.M.M.-A.; Resources, V.Q.A. and F.M.P.; Supervision, V.Q.A. and A.L.C.-V.; Validation, L.L.; Writing – original draft, A.L.C.-V.;Writing—review & editing, J.M.M.-A.

Funding: This research received no external funding.

Acknowledgments: The authors are grateful to Alexis García for his support during the carrying out of the industrial tests and to the Technical Board of the ECCG company for the trust placed in the research team.

Conflicts of Interest: The authors declare no conflict of interest

Appendix A

Table A1. Calculation of the circulating load in the grinding circuit.

Flow of Material, m^3/h	Air Flow, m^3/h	Slope Angle	Size Class, mm	Content of the Class, %			Circulating Load, *C* (*i*)
				Mill Discharge, *f′*	Recirculated Product, *c*	Fine Product, *p*	
+	**+**	**+**	**−0.149 + 0.074**	87.58	54.66	95.66	0.25
			−0.074 + 0.044	79.22	39.70	85.08	0.15
			−0.044 + 0.0	64.13	39.20	75.71	0.46
+	−	−	−0.149 + 0.074	67.67	64.00	97.09	8.01
			−0.074 + 0.044	50.41	44.66	86.92	6.35
			−0.044 + 0.0	44.91	39.03	79.38	5.86
−	+	−	−0.149 + 0.074	81.03	62.71	97.67	0.91
			−0.074 + 0.044	61.31	48.54	88.16	2.10
			−0.044 + 0.0	50.2	42.06	80.34	3.70
−	−	+	−0.149 + 0.074	85.28	49.405	94.06	0.24
			−0.074 + 0.044	69.21	38.41	87.3	0.59
			−0.044 + 0.0	60.56	37.93	73.56	0.57
+	+	−	−0.149 + 0.074	85.34	65.60	97.41	0.61
			−0.074 + 0.044	76.89	46.12	87.17	0.33
			−0.044 + 0.0	53.49	38.73	78.77	1.71
+	−	+	−0.149 + 0.074	70.63	61.04	95.92	2.64
			−0.074 + 0.044	52.58	46.46	84.2	5.16
			−0.044 + 0.0	46.51	39.94	71.33	3.78
−	+	+	−0.149 + 0.074	81.93	51.51	96.29	0.47
			−0.074 + 0.044	66.17	43.86	86.9	0.93
			−0.044 + 0.0	59.77	33.46	74.84	0.57
−	−	−	−0.149 + 0.074	79.46	60.08	97.02	0.91
			−0.074 + 0.044	61.37	22.37	85.1	0.61
			−0.044 + 0.0	53.13	17.18	78.77	0.71

Table A2. Calculation of residuals.

Recalculated Circulating Load					Residual, ε	Lagrange Multiplier, λ
p-f	f-c	$(f\text{-}c)^2$	(p-f)*(f-c)	C (*i*)		
8.08	32.92	1083.73	265.99		−0.16	−0,06
5.86	39.53	1562.23	231.62		3.65	1.41
11.58	24.93	621.50	288.69		−5.58	−2.15
Sum Total		3267.46	786.30	0.24		
29.42	3.68	13.51	108.12		−5.84	−0,06
36.51	5.75	33.06	209.93		0.39	0.00
34.47	5.88	34.57	202.68		3.27	0.03
Sum Total		81.14	520.73	6.42		
16.64	18.33	335.81	304.93		12.32	1.21
26.85	12.77	163.07	342.87		−6.67	−0.66
30.14	8.14	66.26	245.34		−17.28	−1.70
Sum Total		565.14	893.14	1.58		
8.78	35.875	1287.02	314.98		6.45	2.01
18.09	30.8	948.64	557.17		−5.02	−1.56
13	22.63	512.12	294.19		-3.39	−1.06
Sum Total		2747.77	1166.34	0.42		
12.07	19.74	389.67	238.26		−0.29	−0.07
10.28	30.775	947.10	316.37		8.09	2.07
25.28	14.76	217.86	373.13		−16.47	−4.22
Sum Total		1554.63	927.76	0.60		

Table A2. *Cont.*

Recalculated Circulating Load					Residual, ε	Lagrange Multiplier, λ
p-f	f-c	$(f\text{-}c)^2$	(p-f)*(f-c)	C (*i*)		
25.29	9.59	91.97	242.53		8.00	0.24
31.62	6.125	37.52	193.67		−10.36	−0.31
24.82	6.57	43.16	163.07		−2.02	−0.06
Sum Total		172.65	599.27	3.47		
14.36	30.42	925.38	436.83		4.27	1.07
20.73	22.315	497.96	462.59		−7.06	−1.78
15.07	26.315	692.48	396.57		1.05	0.26
Sum Total		2115.81	1295.99	0.61		
17.56	19.385	375.78	340.40		−4.26	−0.99
23.73	39.005	1521.39	925.59		3.02	0.70
25.64	35.955	1292.76	921.89		−0.98	−0.23
Sum Total		3189.93	2187.88	0.69		

Table A3. Recalculated values of the particle size distribution for the grinding circuit products.

Recalculated Class Content, %			Recalculated Residual, ε
Mill Discharge, f.	Recirculated Product, c	Fine Product, p	
87.66	54.65	95.60	0
77.48	40.03	86.49	0
66.80	38.68	73.56	0
68.1	63.6	97.03	0
50.4	44.7	86.92	0
44.7	39.2	79.41	0
77.9	64.6	98.88	0
63.0	47.5	87.50	0
54.6	39.4	78.64	0
82.4	50.3	96.07	0
71.4	37.7	85.74	0
62.1	37.5	72.50	0
85.5	65.6	97.34	0
73.6	47.4	89.24	0
60.2	36.2	74.55	0
69.5	61.9	96.16	0
54.0	45.4	83.89	0
46.8	39.7	71.27	0
80.2	52.2	97.36	0
69.0	42.8	85.12	0
59.3	33.6	75.10	0
81.1	59.4	96.03	0
60.2	22.8	85.80	0
53.5	17.0	78.54	0

References

1. Ouchterlony, F. Fragmentation characterization; the Swebrec function and its use in blast engineering. In Proceedings of the 9th International Symposium on Rock Fragmentation by Blasting—Fragblast 9, Granada, Spain, 13–17 August 2009; pp. 3–22.
2. Coello-Velázquez, A.L. Sovershenstvovanie tecnologii izmilchenii lateritobij pud na zabode "Punta Gorda". Ph.D. Thesis, IMS, Saint Petersburg, Russia, 1993.
3. Aguado, J.M.M.; Velázquez, A.L.C.; Tijonov, O.N.; Díaz, M.A.R. Implementation of energy sustainability concepts during the comminution process of the Punta Gorda nickel ore plant (Cuba). *Powder Technol.* **2006**, *170*, 153–157. [CrossRef]

4. Coello Velázquez, A.L.; Menéndez-Aguado, J.M.; Brown, R.L. Grindability of lateritic nickel ores in Cuba. *Powder Technol.* **2008**, *182*, 113–115. [CrossRef]
5. Chalkley, M.E.; Collins, M.J.; Iglesias, C.; Tuffrey, N.E. Effect of magnesium on pressure leaching of Moa Laterite ore. *Can. Metall. Q* **2010**, *49*, 227–234. [CrossRef]
6. Sanchidrián, J.A.; Ouchterlony, F.; Moser, P.; Segarra, P.; López, L.M. Performance of some distributions to describe rock fragmentation data. *Int. J. Rock Mech. Min. Sci.* **2012**, *53*, 18–31. [CrossRef]
7. Sbarbaro, D.; Ascencio, P.; Espinoza, P.; Mujica, F.; Cortes, G. Adaptive soft-sensors for on-line particles estimation in wet grinding circuits. *Control Eng. Practice.* **2008**, *16*, 171–178. [CrossRef]
8. Ko, Y.-D.; Shang, H. A neural network-based soft sensor for particle size distribution using image analysis. *Powder Technol.* **2011**, *212*, 359–366. [CrossRef]
9. Wills, B.A.; Finch, J.A. *Wills' Mineral Processing Technology: An Introduction to the Practical Aspects of Ore Treatment and Mineral Recovery*, 8th ed.; Elsevier: Amsterdam, The Netherlands, 2016; p. 498.
10. Ouchterlony, F. The Swebrec function: Linking fragmentation by blasting and crushing. Institution of Mining and Metallurgy. *Min. Technol.* **2005**, *114*, 29–44. [CrossRef]
11. Ouchterlony, F.; Moser, P. Likenesses and differences in the fragmentation of full-scale and model-scale blasts. In Proceedings of the 8th International Symposium on Rock Fragmentation by Blasting–Frag blast 8, Santiago, Chile, 7–11 May 2006; pp. 207–220.
12. Álvarez Rodríguez, B.; González García, G.; Coello-Velázquez, A.L.; Menéndez-Aguado, J.M. Product size distribution function influence on interpolation calculations in the Bond ball mill grindability test. *Int. J. Miner. Process.* **2016**, *157*, 16–20. [CrossRef]
13. Kelly, E.G.; Spottiswood, D.J. *Introduction to Mineral Processing*; John Willey and Sons: Hoboken, NJ, USA, 1982.
14. Blair, D.P. Curve-fitting schemes for fragmentation data. *Fragblast. Int. J. Blast. Fragment.* **2004**, *8*, 137–150.
15. Kuznetsov, V.M. The mean diameter of the fragments formed by blasting rock. *Sov. Min. Sci.* **1973**, *9*, 144–148. [CrossRef]
16. Djordjevic, N. Two-component model of blast fragmentation. In Proceedings of the 6th International Symposium on Rock Fragmentation by Blasting, Johannesburg, South Africa, 8–12 August 1999; pp. 213–219.
17. Kanchibotla, S.S.; Valery, W.; Morell, S. Modelling fines in blast fragmentation and its impact on crushing and grinding. In Proceedings of the Conference on Rock Breaking, Kalgoorlie, WA, USA, 7–11 November 1999; pp. 137–144.
18. Osorio, A.M.; Menéndez-Aguado, J.M.; Bustamante, O.; Restrepo, G.M. Fine grinding size distribution analysis using the Swebrec function. *Powder Technol.* **2014**, *258*, 206–208. [CrossRef]
19. Coello-Velázquez, A.L. Procedimiento para la determinación de la carga circulante en circuitos cerrados de trituración y molienda. *Minería y Geología* **2015**, *31*, 66–79.
20. Menéndez-Aguado, J.M.; Coello, A.L.; Tikjonov, O.N.; Rodríguez, M. Implementation of sustainable concepts during comminution process in Punta Gorda nickel ore plant. *Powder Technol.* **2006**, *170*, 153–157. [CrossRef]